Available online at www.sciencedirect.com
ScienceDirect
Journal of Photochemistry and Photobiology A: Chemistry 191 (2007) 32–41
Journal of Photochemistry and Photobiology A:Chemistry
www.elsevier.com/locate/jphotochem

Charge transfer fluorescence of benzoxazol derivatives Investigation of solvent effect on fluorescence of these dyes

Marek Mac [a,*], Bogdan Tokarczyk [a], Tomasz Uchacz [a], Andrzej Danel [b]

[a] *Faculty of Chemistry, Jagiellonian University, Ingardena 3, 30-060 Kraków, Poland*
[b] *Department of Chemistry, University of Agriculture, Balicka 122, 31-149 Kraków, Poland*

Received 28 December 2006; received in revised form 2 April 2007; accepted 2 April 2007
Available online 5 April 2007

Abstract

Fluorescence of derivatives containing the *N*,*N*-dimethylaniline group attached to 2-phenyl-benzoxazole via double-bounded spacer shows extremely strong dependence of the position of the fluorescence maximum on solvent polarity. This indicates a strong charge transfer character of the emitting singlet state of these dyes. Electron transfer parameters such as solvent dependent reorganization energies and free energy changes for the back electron transfer process have been estimated from the analysis of the charge transfer fluorescence spectra. Surprisingly, the internal reorganization energy decreases with increasing solvent polarity. The same trend shows the values of the internal reorganization energy estimated from the temperature fluorescence measurements. This may indicate that the electronic structure of the dye has a biradical character already in the ground state in polar solvents. It has been also found that major channel of the nonradiative deactivation of the excited singlet state is an isomerisation of the compound leading to the isomer *cis*.

Keywords: Electron transfer; CT fluorescence; *trans–cis* isomerisation; Nonradiative transitions

1. Introduction

Fluorescence techniques are recently used for detection of small amounts of inorganic species in solution, especially metal cations [1]. The design of fluorescent sensors is of major importance due to their application in analytical chemistry, clinical biochemistry, medicine, the environment, etc. Even small amounts of chemical and biochemical substances can be detected by fluorescence methods: cations, anions, neutral molecules and gases. Although there is already a wide choice of fluorescent molecular sensors for particular applications there is still a need for sensors with improved selectivity and minimum perturbation of the microenvironment to be probed. Among the fluorescent sensors a monomolecular charge transfer systems play an important role. The principle of working of such sensors is as follows: the cation receptor is an azacrown system connected to the electron accepting group. In the absence of cation, which may be bounded to the azacrown moiety, the electron–donor–acceptor (EDA) molecule exhibits a property of the charge transfer system. Upon complexation by inorganic cation the electron donating ability of electron donor drops down and the system does not exhibit charge transfer character. The absorption is thus shifted hypsochromically compared to that of the uncomplexed system. Ostensibly understandable is a very weak hypsochromic shift of the fluorescence spectrum of the complexed systems. It may be explained in the following way: the excitation makes the electron donating part of the molecule positively charged thus a disruption of the nitrogen-cation bound exists making the fluorescence very similar to that of the uncomplexed system. The charge transfer systems which contain donor–acceptor subunits connected with a double bond system are also frequently used as cation indicators. A good candidate for such fluorescent sensor are the E–D–A systems containing the benzoxazole subunit. Some recent papers [2,3] showed that benzoxazole derivatives bind the Zn^{2+} and Mg^{2+} cations forming the stable complexes of 1:1 stoichometry. It has been also found that benzoxazole derivatives are good materials for applications as full colour flat-pannel displays [4]. Their fluorescence properties are affected by substitution of the electrondonating or electroaccepting groups. It has been also found that changing of solvent influences fluorescence properties of the materials. This makes benzoxazole deriva-

* Corresponding author. Tel.: +48 12 6632262; fax: +48 12 6340515.
E-mail address: mac@chemia.uj.edu.pl (M. Mac).

1010-6030/$ – see front matter © 2007 Elsevier B.V. All rights reserved.
doi:10.1016/j.jphotochem.2007.04.001

tives interesting substances in basic photophysical investigations.

On the other hand, *trans–cis* photoisomerisation of the compounds containing double bond was also thoroughly studied [5,6]. An example is a large class of stilbenes, in which photoreactivity was investigated as a function of reactant's properties such as electrodonating character of substituents and influence of solvent polarity [7,8]. This affects a charge distribution in the excited states of these molecules. It has been found that isomerisation may occur in the excited singlet state for parent stilbene and cyano-dimethylaminostilbene but introduction of the nitro group changes isomerisation mechanism and now it proceeds in the triplet state [9]. Fayed et al. investigated the fluorescence behaviour and *trans–cis* isomerisation of some *trans* 2-styrylbenzoxazoles [10,11], including 2-(*p*-dimethylaminostyryl)benzoxazole. They found that this compound in the excited singlet state exhibits a CT character as can be judged from the large Stokes shift with increasing solvent polarity. The quantum yields of fluorescence are rather low (below 0.02 in low viscous solvents) and they did not show changes with solvent polarity alteration, however in solvents of high viscosity the fluorescence quantum yield significantly increases. Similar behaviour has been observed for the *trans–cis* isomerisation quantum yield. It has been found that the fluorescence quantum yield depends strongly on temperature. Introduction of one phenyl ring into this moiety changes the fluorescence properties a lot, therefore we decided to investigate the substances containing a phenyl benzoxazole system presented in Fig. 1.

We focused our attention on the compounds having benzoxazole subunit connected with *N*,*N*-dimethylaniline via π-conjugated chain containing one or two double bonds. Additionally, we have investigated the mechanism of the *trans–cis* isomerisation of {4-[(*E*)-2-(4-benzoxazol-2-yl-phenyl)-vinyl] -phenyl}-dimethylamine (system **II**). Also, the possibility of azacrown containing system, i.e. 2-(4-{(*E*)-2-[4-(1,4,7,10-tetraoxa-13-aza-cyclopentadec-13-yl)-phenyl]-vinyl}phenyl)-benzoxazole has been checked as a potential fluorescing indicator of small cations (system **IV**).

2. Experimental

The synthetic procedure of the stilbene (**I–IV**) syntheses is depicted in Fig. 1. Thus, the benzoxazole **3** was prepared by condensation of *o*-aminophenol **1** with *p*-toluic acid **2** in polyphosphoric acid (PPA) [12]. Bromomethyl derivative **4** was obtained by bromination of **3** with *N*-bromosuccinimide (NBS). Compound **4** was transformed into **5** by heating it with an excess of triethyl phosphite. Stilbene derivatives (**II–IV**) (i.e. except for **I**) were prepared by Horner–Wittig procedure by reacting of **5** with aromatic aldehydes in 1-methyl-2-pyrrolidinone (NMP) and potassium *tert*-butoxide.

^{1}H NMR spectra were recorded on a Mercury-Vx 300 MHz Varian. Melting points were measured on a Melt-temp apparatus. Chemicals were purchased from commercial suppliers (Merck or Aldrich). Elemental analyses were in good agreement with calculated values (±0.3%).

2.1. 2-(p-Bromomethylphenyl)-benzoxazole *4*

Compound **3** (2 g, 0.01 mol), NBS (2.13 g, 0.012 mol) and 50 mg of azobisisobutyronitrile (AIBN) were dissolved in 50 mL

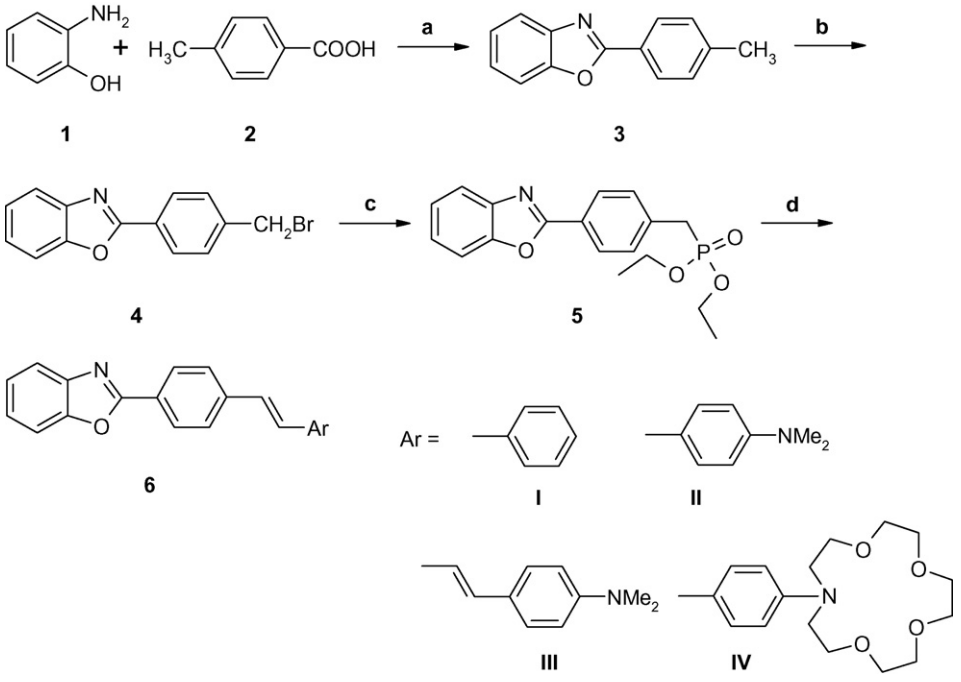

Fig. 1. Chemical names of the compounds of our interest (**I–IV**). 2-(4-(*E*)-Styrylphenyl)-benzoxazole **I**, {4-[(*E*)-2-(4-benzoxazol-2-yl-phenyl)-vinyl]-phenyl}-dimethylamine **II**, {4-[(1*E*,3*E*)-4-(4-benzoxazol-2-yl-phenyl)-buta-1,3-dienyl]-phenyl}-dimethylamine **III**, and 2-(4-{(*E*)-2-[4-(1,4,7,10-tetraoxa-13-aza-cyclopentadec-13-yl)-phenyl]-vinyl}phenyl)-benzoxazole **IV**. (a) PPA, 110–120 °C; (b) NBS; (c) $P(OEt)_3$; (d) *t*-BuOK/NMP.

of anhydrous CCl_4 and boiled for 8 h. The hot reaction mixture was filtered to remove succinimide and evaporated. The crude compound was crystallized from toluene.

Colourless crystals, mp 149 °C, 1.9 g, yield 67%.

^{1}H NMR (300 MHz, $CDCl_3$, δ ppm): 8.18 (d, J = 8.4 Hz, 2H), 7.78–7.72 (m, 1H); 7.63 (d, J = 8.4 Hz, 2H); 7.60–7.57 (m, 1H); 7.38–7.35 (m, 2H); 4.57 (s, 2H, $-CH_2-$).

2.2. Diethyl (4-benzoxazol-2-yl benzyl)-phosphonate **5**

Compound **4** (5.7 g, 0.02 mol) and an excess of triethyl phosphite were heated at 160 °C for 12 h. Unreacted triethyl phosphite was removed under reduced pressure and the brownish oily residue was dissolved in toluene and subjected to column chromatography on silica gel (Merck 60, 70–230 mesh) using toluene/ethyl acetate 3:1 and ethyl acetate at the end of elution.

Colourless crystals, mp 60 °C, 4.7 g, yield 69%.

^{1}H NMR (300 MHz, $CDCl_3$, δ ppm): 8.18 (d, J = 7.41 Hz, 2H), 7.75–7.72 (m, 1H); 7.57–7.52 (m, 1H); 7.44 (dd, J = 8.6; 2.5 Hz, 2H); 7.34–7.31 (m, 2H); 4.02 (q, 4H); 3.22 (d, J = 22.3 Hz, 2H); 1.24 (t, 6H).

2.3. 2-(4-(E)-Styrylphenyl)-benzoxazole **I**

Compound was prepared according to the literature procedure developed by Siegrist [12].

2.4. {4-[(E)-2-(4-Benzoxazol-2-yl-phenyl)-vinyl]-phenyl}-dimethylamine **II**

Potassium *tert*-butoxide (1.22 g, 0.01 mol) was added to a solution of the phosphonate compound **5** (3.5 g, 0.01 mol) in dry dimethoxyethane (20 mL) at room temperature. The resulting yellow-orange solution was stirred for 15 min. Then, 4-*N*,*N*-dimethylbenzaldehyde (1.49 g, 0.01 mol) was added. The solution, which turned a very intense deep purple colour, was stirred for 1 h. The final suspension was quenched with HCl (10%, 10 mL) to give a yellow suspension that was stirred for 1 h. The precipitate was filtered off, washed with water, and dried. Pure compound was obtained by chromatography (silica gel, Merck 60, 70–230 mesh, toluene/ethyl acetate 3:1).

Yellow crystals, mp 256 °C, 1.2 g, yield 35%.

^{1}H NMR (300 MHz, $CDCl_3$, δ ppm): 8.23 (d, J = 8.4 Hz, 2H); 7.79–7.77 (m, 1H); 7.63 (d, J = 8.4 Hz, 2H); 7.60–7.58 (m, 1H); 7.47 (d, J = 8.5 Hz, 2H); 7.38–7.34 (m, 2H); 7.21 (d, J = 16.2 Hz, 1H); 6.97 (d, J = 16.2 Hz, 1H); 6.77 (s broad, 2H); 2.95 (s, 6H, NMe_2).

Compounds **III** and **IV** were prepared according to the synthetic procedure of **II**.

2.5. {4-[(1E,3E)-4-(4-Benzoxazol-2-yl-phenyl)-buta-1,3-dienyl]-phenyl}-dimethylamine (**III**)

Orange needless, mp 285 °C, yield 56%.

^{1}H NMR (300 MHz, $CDCl_3$, δ ppm): 8.22 (d, J = 8.4 Hz, 2H); 7.81–7.78 (m, 1H); 7.64–7.57 (m, 3H); 7.41–7.36 (m, 4H); 7.16–7.07 (m, 1H); 6.85–6.62 (m, 5H).

2.6. 2-(4-{(E)-2-[4-(1,4,7,10-Tetraoxa-13-aza-cyclopentadec-13-yl)-phenyl]-vinyl}phenyl)-benzoxazole (**IV**)

Yellow crystals, mp 160 °C, yield 43%.

^{1}H NMR (300 MHz, $CDCl_3$, δ ppm): 8.24 (d, J = 8.43 Hz, 2H); 7.81–7.78 (m, 1H); 7.66–7.60 (m, 3H); 7.46 (d, J = 8.7 Hz, 2H); 7.39–7.36 (m, 2H); 7.21 (d, J = 15.9 Hz, 1H); 6.98 (d, J = 16.7 Hz, 1H); 6.74–6.71 (m, 2H); 3.83 (t, 4H); 3.71–3.68 (m, 16H).

Fluorescence arrangement was described in the previous paper [13]. The samples (prepared in the darkness) were degassed before experiments using the freezing–pumping–thawing technique. The fluorescence quantum yields were determined from the steady-state measurements, from the corrected for spectral sensitivity fluorescence spectra using quinine sulphate in 0.01 H_2SO_4 as an actinometer (Φ_{fl} = 0.55). The fluorescence lifetimes were estimated from the decay curves measured by time-resolved single photon counting. As an excitation source a picosecond diode laser (λ = 400 nm, 70 ps pulse duration) or nanosecond diode (λ = 370 nm, 1 ns pulse duration) (both from IBH-UK) were used. Analysis of the decay functions were performed by a convolution method using the own FORTRAN programs.

The CT fluorescence analysis was done using the equation for the charge transfer fluorescence distribution. For minimisation procedure the MINUITS packet from the CERN Library was applied.

trans–cis isomerisation process (only for compound **II**) was monitored by measuring the absorption spectra of the compound upon irradiation of the sample by a 405 nm line of a Hg lamp equipped by a suitable monochromator. As a reference the *trans–cis* isomerisation of *trans*-4-dimethylamino-4′-nitrostilbene in cyclohexane was applied (Φ_{t-c} = 0.45) [14]. To determine the quantum efficiency of isomerisation the method described by Gauglitz and Hubig was applied [15].

3. Results

3.1. Absorption and fluorescence measurements

Absorption and fluorescence spectra of the compounds **I–IV** in acetonitrile are presented in Fig. 2.

In *n*-hexane absorption and fluorescence of the compounds **I–IV** show a vibrational structure whereas in more polar solvents it vanishes for the systems containing the dimethylaniline and azacrown subunits (i.e. in compounds **II–IV**). We observe clearly batochromic shift both in absorption and fluorescence going from 2-(4′-methylphenyl)benzoxazole (which is a pattern molecule of the electron acceptor in the investigated systems (**I–IV**)) to the π-conjugated systems. Changing solvent polarity causes a small alteration of the absorption and emission spectra of the compound **I**. Contrary to **I**, the compounds containing electrodonating groups show large solvatochromic shift in fluorescence and much smaller in absorption (both batochromic). This large solvatochromic shift in the fluorescence is a result of the intramolecular charge transfer process leading to the full

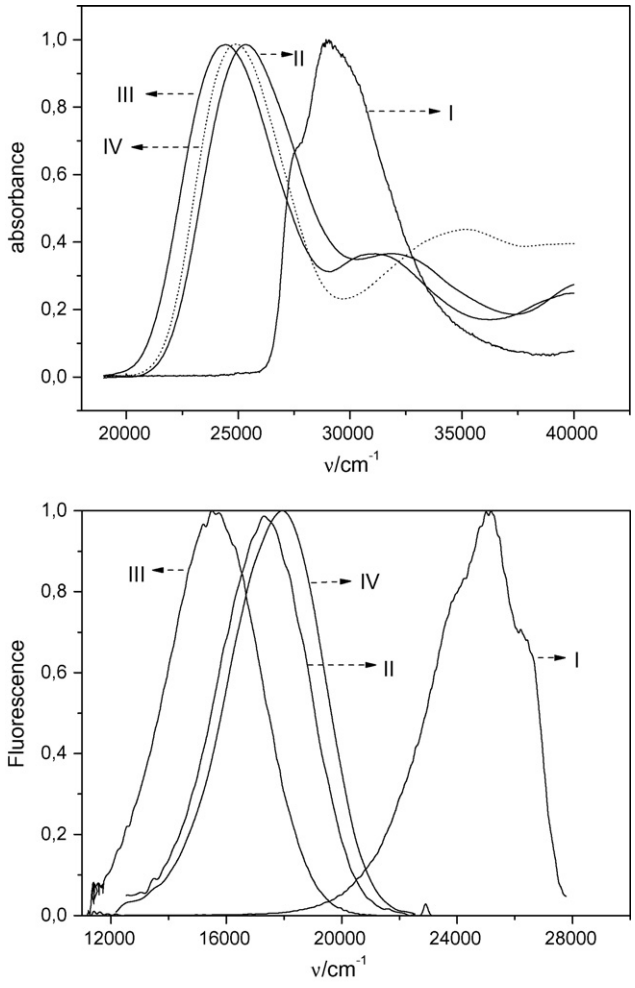

Fig. 2. Normalized absorption (top) and emission (bottom) spectra of the compounds **I–IV** in acetonitrile.

separation of the charges in the excited singlet state. The representative fluorescence spectra of **II** in selected solvents are presented in Fig. 3.

The spectral shift of the fluorescence maximum, or more strictly, the difference between the positions of the absorption and fluorescence maximum depends on solvent polarity function defined by dielectric constant and reflective index of the solvent. For such a biradical-type state the dipole moment change connected with an intramolecular charge transfer process can be experimentally calculated from the Lippert–Mataga relationship, neglecting a mean solute polarizability ($\alpha \approx \alpha_e \approx \alpha_g \approx 0$) [16]:

$$h\nu_{abs} - h\nu_{fl} = m_1 f(n^2, \varepsilon_s) = \frac{(\vec{\mu}_e - \vec{\mu}_g)^2}{2\pi\varepsilon_0 hca^3} f(n^2, \varepsilon_s)$$

$$= \frac{(\vec{\mu}_e - \vec{\mu}_g)^2}{2\pi\varepsilon_0 hca^3} \left(\frac{\varepsilon_s - 1}{2\varepsilon_s + 1} - \frac{n^2 - 1}{2n^2 + 1} \right) \quad (1a)$$

where μ_e and μ_g are the dipole moments of the fluorophore in the excited and the ground state, respectively; a is a radius of the Onsager cavity, assumed to be a sphere.

The representative Lippet–Mataga plot for the compound **II** is presented in Fig. 4.

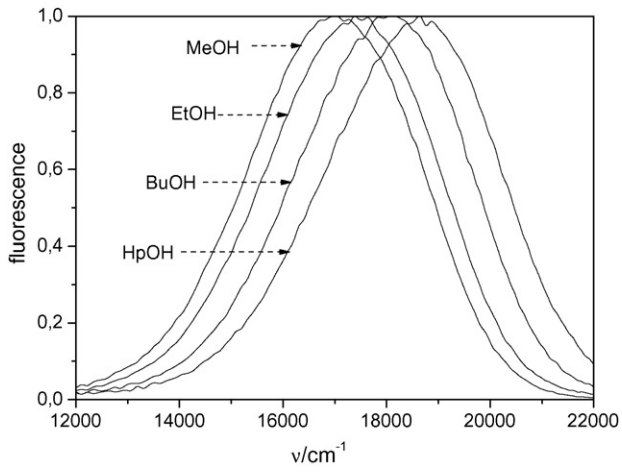

Fig. 3. Corrected for spectral sensitivity and normalized fluorescence spectra of **II** in *n*-heptanol (HpOH), *n*-butanol (BuOH), ethanol (EtOH) and methanol (MeOH) taken at room temperature upon excitation by a 405 nm Hg-line.

A similar linear dependence can be found for the sum of the position of the maximum of the first absorption band and that of fluorescence on another function of solvent polarity [17]. This equation is also valid when we neglect the polarizability of the solute and with the assumption that the Onsager cavity can be approximated by a sphere of radius a:

$$h\nu_{abs} + h\nu_{fl} = m_2[f(n^2, \varepsilon_s) + 2g(n)]$$

$$= \frac{(\vec{\mu}_e^2 - \vec{\mu}_g^2)}{2\pi\varepsilon_0 hca^3}[f(n^2, \varepsilon_s) + 2g(n)]$$

$$= \frac{(\vec{\mu}_e^2 - \vec{\mu}_g^2)}{2\pi\varepsilon_0 hca^3} \left(\frac{\varepsilon_s - 1}{2\varepsilon_s + 1} + \frac{n^2 - 1}{2n^2 + 1} \right) \quad (1b)$$

Assuming that the dipole moment in the ground state is equal to 5.75 D (*ab initio* calculations) we are able to calculate the dipole moment in the excited singlet state and the angle ϕ between the dipole moments using the following equations [17]:

$$\mu_e = (\mu_g^2 + 2m_2\pi\varepsilon_0 hca^3)^{1/2} \quad (1c)$$

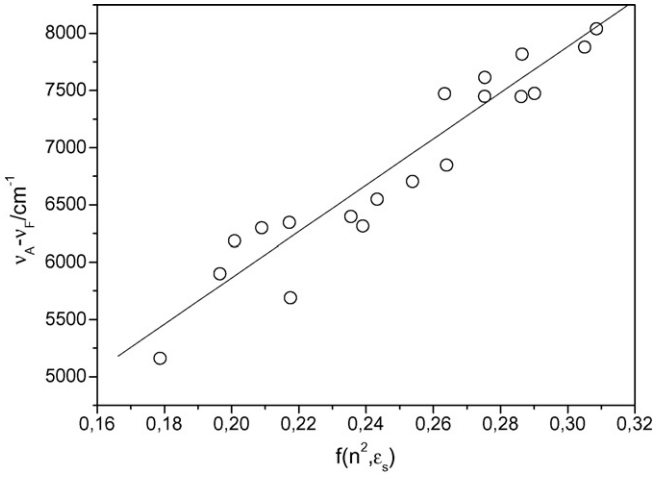

Fig. 4. Lippert–Mataga plot of the difference between the maximum of the CT-absorption and fluorescence on the solvent-polarity function $f(n^2,\varepsilon_s) = (((\varepsilon_s - 1)/(2\varepsilon_s + 1)) - ((n^2 - 1)/(2n^2 + 1)))$ for the compound **II**.

Table 1
Photophysical properties of **II**, **III** and **IV** in solvents of various polarity

Solvent	ε_s	η (MPa s)	Φ_{fl}	τ_{fl} (ns)	k_{rad} ($\times 10^9$ s^{-1})	ν_{max} (cm^{-1})	k_{nr} ($\times 10^9$ s^{-1})
HEX	1.88	0.3	0.364	0.55	0.66	–	1.15
DBE	3.11	0.637	0.32	0.61	0.52	21,160	1.11
EtAC	6.09	0.423	0.42	0.91	0.46	19,240	0.63
THF	7.52	0.456	0.465	1.06	0.44	18,960	0.50
EtBr	9.01	0.374	0.41	0.87	0.47	19,290	0.67
EtI	7.82	0.556	0.5	0.87	0.57	19,290	0.57
PrOH	20.8	1.945	0.51	1.51	0.34	17,810	0.32
CHXOH	16.4	57.5	0.60	1.13	0.53	18,580	0.35
$MeCl_2$	8.93	0.413	0.42	1.07	0.39	18,780	0.54
GTA	7.3		0.53	1.47	0.36	18,960	0.32
ACE	20.7	0.306	0.52	1.42	0.37	17,850	0.34
ACN	37.5	0.369	0.51	1.61	0.32	17,380	0.30
DMF	38.25	0.794	0.68	1.64	0.41	17,310	0.20
PC	66.14		0.68	1.85	0.37	17,200	0.17
DMSO	47.24	1.987	0.95	1.86	0.51	16,860	0.03
EtAc	6.09	0.423	0.42	0.98	0.43	17,380	0.57
THF	7.52	0.456	0.47	0.85	0.55	17,340	0.62
EtBr	9.01	0.374	0.46	0.84	0.55	17,390	0.67
EtI	7.82	0.556	0.47	0.84	0.56	17,310	0.63
PrOH	20.8	1.945	0.49	1.38	0.35	16,170	0.37
CHXOH	16.4	57.5	0.41	1.16	0.35	16,870	0.51
$MeCl_2$	8.93	0.413	0.46	0.94	0.49	17,050	0.57
GTA	7.3		0.57	1.34	0.42	17,300	0.32
ACE	20.7	0.306	0.46	1.31	0.35	16,060	0.41
ACN	37.5	0.369	0.63	1.52	0.41	15,640	0.24
DMF	38.25	0.794	0.66	1.62	0.41	15,600	0.21
PC	66.14		0.71	1.80	0.4	15,360	0.16
DMSO	47.24	1.987	0.98	1.89	0.52	15,130	0.01
HEX	1.88	0.3	0.28	0.53	0.55		1.35
EtAc	6.09	0.423	0.39	1.0	0.39	19,430	0.71
EtBr	9.01	0.374	0.32	0.9	0.36	19,420	0.8
EtI	7.82	0.556	0.37	0.9	0.41	19,470	0.7
PrOH	20.8	1.945	0.52	1.51	0.34	17,810	0.32
CHXOH	16.4	57.5	0.6	1.31	0.45	18,820	0.31
$MeCl_2$	8.93	0.413	0.47	1.1	0.43	19,010	0.48
GTA	7.3		0.55	1.54	0.36	19,080	0.29
ACE	20.7	0.306	0.57	1.33	0.43	18,280	0.32
ACN	37.5	0.369	0.58	1.50	0.39	17,780	0.28
PC	66.14		0.59	1.65	0.36	17,600	0.25
DMSO	47.24	1.987	0.90	1.83	0.49	17,270	0.05

The used symbols have following meanings—ε_s: dielectric permittivity of the solvent; Φ_{fl}: absolute quantum yield of the fluorescence; τ_{fl}: the fluorescence lifetime; measured at fluorescence maximum ν_{max}; k_{rad}: radiative charge transfer rate constant, defined as Φ_{fl}/τ_{fl}; ν_{max}: position of the maximum of the charge transfer fluorescence band. Viscosity parameters of the solvents were taken from Refs. [18,19] and refer to 25 °C.
Solvents—HEX: *n*-hexane; DBE: dibutylether; EtAc: ethyl acetate; THF: tetrahydrofuran; EtBr: ethyl bromide; EtI: ethyl iodide; PrOH: *n*-propanol; CHXOH: cyclohexanol; $MeCl_2$: methylene chloride; GTA: glycerol triacetate; ACE: acetone; CAN: acetonitrile; DMF: dimethylformamide; PC: propylene carbonate; DMSO: dimethyl sulfoxide.

$$\cos\phi = \frac{1}{2\mu_e\mu_g}\left(\mu_g^2 + \mu_e^2 - \frac{m_1}{m_2}(\mu_e^2 - \mu_g^2)\right) \quad (1d)$$

In the considered case the calculated values of the excited state dipole moment and the angle between the ground and excited state dipole moments are equal to 26.3 D and 46.4°, respectively. It seems that the dipole moments are not collinear.[1]

Alteration of solvent parameters such as polarity and/or viscosity causes significant changes in the photophysical parameters of the molecules as presented for the compounds **II**, **III** and **IV** in Table 1.

As we can see, significant changes of various photophysical properties of the molecules against solvent polarity and/or viscosity parameters have been detected.

3.2. Electron transfer parameters

The above-described effects show undoubtedly that the emission of **II**–**IV** in solvents of medium and high polarities has a

[1] These values are strongly dependent on the choice of some parameters such as: polarizability of the molecule, ground state dipole moment and shape of the Onsager cavity (i.e. sphere or ellipsoid). We decided to use the simplest model (i.e. the Lippert–Mataga model).

character of radiative back electron transfer process (i.e. a process which recovers the ground state molecule on the radiative way). Thus, the band shape analysis may be performed in terms of the Marcus' radiative back electron transfer theory [20]. For charge transfer fluorescence the fluorescence profile is described by the multi-Gaussian function as follows [21]:

$$CT(\nu) = n^3\nu^3\left(\frac{n^2+2}{3}\right)^2\frac{64\pi^2}{3h^3}M^2\sum_{j=0}^{\infty}\frac{S^j}{j!}(4\pi\lambda_s kT)^{-1/2} \times \exp\left(-\frac{(\Delta G_{et} + jh\nu_v + \lambda_s + h\nu)^2}{4\lambda_s kT}\right) \quad (2a)$$

It should be noted that upon normalization of the CT spectrum to its maximal intensity Eq. (2a) converts into a simpler one:

$$CT(\nu) = \nu^3\sum_{j=0}^{\infty}\frac{S^j}{j!}\exp\left(-\frac{(\Delta G_{et} + jh\nu_v + \lambda_s + h\nu)^2}{4\lambda_s kT}\right) \quad (2b)$$

where λ_s is the external reorganization energy, described for monomolecular CT systems [22] as

$$\lambda_s = \frac{\Delta\vec{\mu}^2}{4\pi\varepsilon_0 hca^3}\left(\frac{\varepsilon_s - 1}{2\varepsilon_s + 1} - \frac{n^2-1}{2n^2+1}\right) \quad (3a)$$

The parameters which appear in Eq. (2a) have the following meanings: $S\,(=\lambda_{in}/h\nu_v)$ is the displacement parameter connected with the internal reorganization energy (λ_{in}) and single averaged high-frequency skeletal mode of frequency (ν_v), and ΔG_{et} is the free energy change for the back electron transfer recombination of the radical ions. Parameter M is the transition dipole moment, connected with the electronic coupling matrix element V_0, dipole moment change $\Delta\mu$, and the averaged emission frequency ν_{av} (defined as $\nu_{av} = \int I(\nu)\nu\,d\nu/\int I(\nu)d\nu$) via relation:

$$M = V_0\frac{\Delta\mu}{hc\nu_{av}} \quad (3b)$$

An important parameter which is decisive in electron transfer processes is the electronic coupling between the interacting states, V_0. It has been shown that this parameter may be easily obtained from the static and time-resolved fluorimetric measurements in the following way.

Obtained from the fluorescence quantum yields and the lifetimes values of the radiative deactivation rate constant k_{rad}, may be used for calculations of the transition dipole moment for fluorescence (M) as pointed out below [23]:

$$k_{rad} = \frac{\Phi_f}{\tau_{fl}} = \frac{1}{3.1887\times10^6}(n\nu_{av})^3M^2 \quad (4)$$

Application of Eq. (3b) allows to determine the electronic coupling parameter V_0 (Eq. (3b)).

The calculated values of V_0 scatter around a mean value of 0.19 eV.

First, we would like to discuss the influence of solvent polarity on the charge transfer process employing the Marcus theory for radiative electron transfer process (Eq. (2a)). The electron transfer parameters estimated from this equation are presented in Figs. 5 and 6.

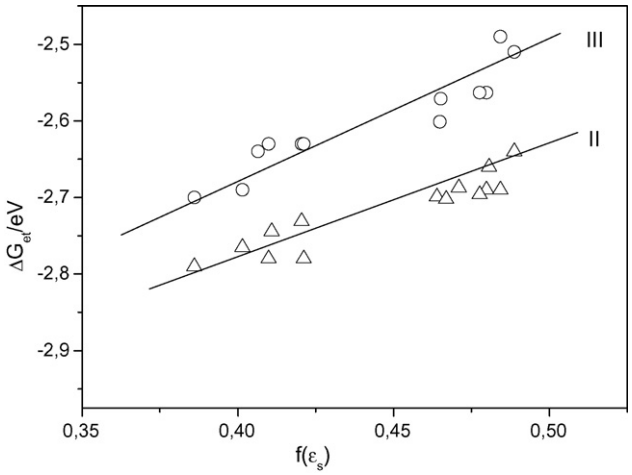

Fig. 5. Dependence of the free enthalpy change for the transition ^{1}CT ⇒ ground state on the solvent polarity function $f(\varepsilon_s) = ((\varepsilon_s - 1)/(2\varepsilon_s + 1))$ for compounds **II** and **III**.

This result is in reasonable agreement with the predictions given by the following equation [22]:

$$\Delta G_{CT} = \Delta G_{CT}\,(\text{vacuum}) - \frac{\vec{\mu}_e^2 - \vec{\mu}_g^2}{4\pi hc\varepsilon_0 a^3}\left(\frac{\varepsilon_s - 1}{2\varepsilon_s + 1}\right) \quad (5)$$

where ΔG_{CT} (vacuum) is the free energy change extrapolated to the gas phase. The other parameters appearing in the above equation were defined previously. This equation predicts a reduction of the energy gap when the solvent polarity increases. Analogous behaviours are found for other CT compounds investigated here (**III** and **IV**).

According to Eq. (3a) increasing solvent polarity causes an increase of the external reorganization energy. The dependence presented in Fig. 6 is not linear, it tends to saturate for solvents of low polarity (DBE).

We can see that introducing a second double bond causes a decrease of the energy gap between the charge transfer and the

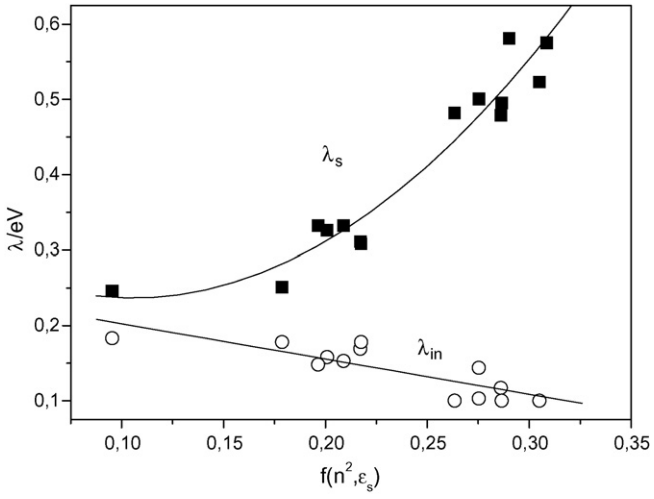

Fig. 6. Dependence of external reorganization energy (λ_s) and internal reorganization energy (λ_{in}) on the solvent polarity function $f(n^2, \varepsilon_s) = (((\varepsilon_s - 1)/(2\varepsilon_s + 1)) - ((n^2 - 1)/(2n^2 + 1)))$ for compound **II**.

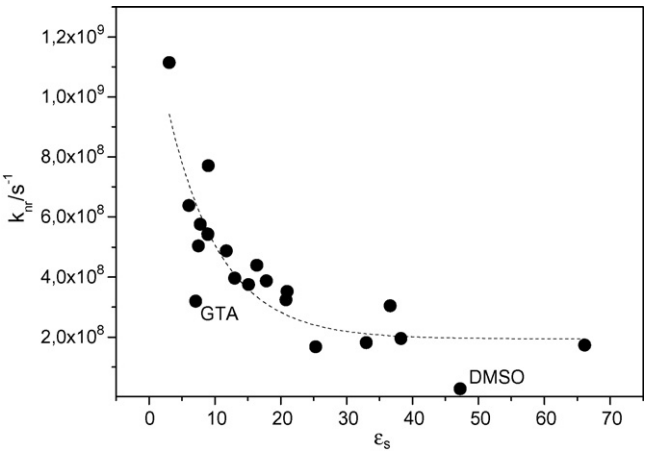

Fig. 7. Dependence of the nonradiative deactivation rate constant of **II** on dielectric permittivity. The correlation line is drawn only for presentation purposes.

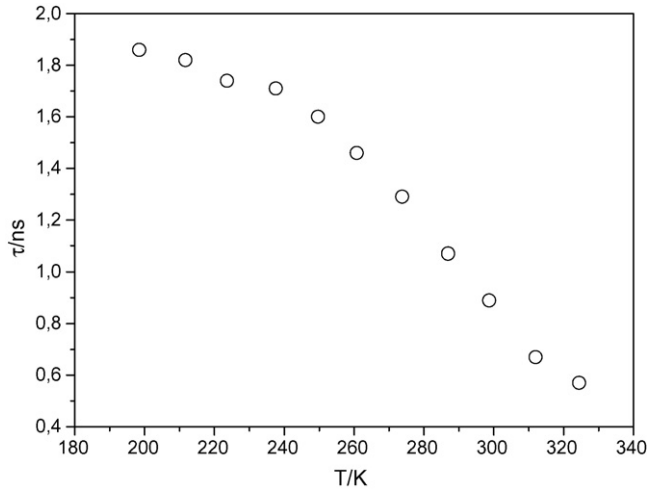

Fig. 8. Dependence of the fluorescence lifetime of **II** in ethyl acetate on temperature.

ground states (cf. Fig. 5). Additionally, it has been found that the solvent reorganization energy is somewhat greater for compound **III**. The second observation indicates a larger separation between the center of the radicals formed in the primary electron transfer process yielding a larger excited state dipole moment in the compound **III**.

As we can notice in Table 1 the rate constant for nonradiative transitions depends strongly on solvent polarity and/or on viscosity of the solvent. Dependence of this quantity on the solvent polarity for compound **II** is presented in Fig. 7.

We can see very clearly that the rate constant of the nonradiative transition decreases with increasing solvent polarity. The effect of decreasing of this quantity is caused at least in part by the increasing viscosity of the solvent (points indicated by acronyms GTA (glycerol triacetate) and DMSO (dimethyl sulfoxide)).

3.3. Temperature measurements of the fluorescence of *II*

Changing of the viscosity and polarity of the medium may be achieved also by alteration of temperature. We performed the measurements of the fluorescence lifetimes of **II** in ethyl acetate at different temperatures. We found a strong increase of this quantity with the decrease of temperature as pointed out in Fig. 8.

An important result emerges from the data obtained from the analysis of the charge-transfer fluorescence profiles according to the Marcus theory (Eq. (2b)). We found a significant decrease of the internal reorganization energy with increasing solvent polarity (cf. Fig. 6). That was a surprising result because for other systems investigated by us this parameter was not sensitive to solvent polarity change. To verify this finding, which emerges from the nonlinear minimization procedure (yielding always uncertaintities in the parameter's estimation), we measured the fluorescence spectra of **II** in some solvents of different polarity (dibutyl ether, methylene dichloride, acetone and dimethyl formamide) at various temperatures. In all cases we observed the hypsochromic shift of the position of fluorescence maximum ($h\nu_{max}$) with increasing temperature. The detailed inspection in the experimental data shows also that with increasing temperature the bandwidth ($\Delta\nu_{1/2}$) of the CT fluorescence is increased. Both quantities ($h\nu_{max}$ and $\Delta\nu_{1/2}$) are connected with important parameters which characterize the transition from ^{1}CT to the ground state [24]:

$$h\nu_{max} = A + BT = A + T\left(\Delta S - \frac{\delta\lambda_s}{\delta T}\right) \tag{6a}$$

$$\frac{(h\Delta\nu_{1/2})^2}{8\ln 2} = C + DT = 2\lambda_s kT + \lambda_i h\langle\omega_v\rangle \tag{6b}$$

The plots of the above-introduced parameters versus temperature for the system **II** in DBE and $MeCl_2$ are presented below (Fig. 9).

As we expected the slope of the dependence of the position of the CT fluorescence maximum on temperature is greater for polar solvents (DMF, acetone $9–10 \times 10^{-4}$ eV/K) than in weakly polar DBE (5.3×10^{-4} eV/K). This points out to a greater entropy change which accompanies the transition from the highly polar excited state to the less polar ground state. The second dependence (Eq. (6b)) allows us to determine the high-frequency internal reorganization energy from the easily accessible (and thus reliable) values of the half-width of the charge transfer fluorescence spectrum. The value of the abscissa, which determines the value of the internal reorganization energy, decreases when the solvent polarity increases (0.176, 0.134, 0.12 and 0.11 eV for DBE, $MeCl_2$, acetone and DMF, respectively).

The values of the internal reorganization energy obtained from the fluorescence band shape analysis (nonlinear regression method) differ slightly from the values obtained from the half-width of the charge transfer fluorescence. The reason of this small discrepancy may be the assumption of the invariance of the solvent reorganization energy with temperature (Eq. (6b)). However, the trend in this tendency remains the same; increasing solvent polarity creates smaller intramolecular changes (i.e. atom–atom distances and the angles between bonds in the molecule) upon excitation.

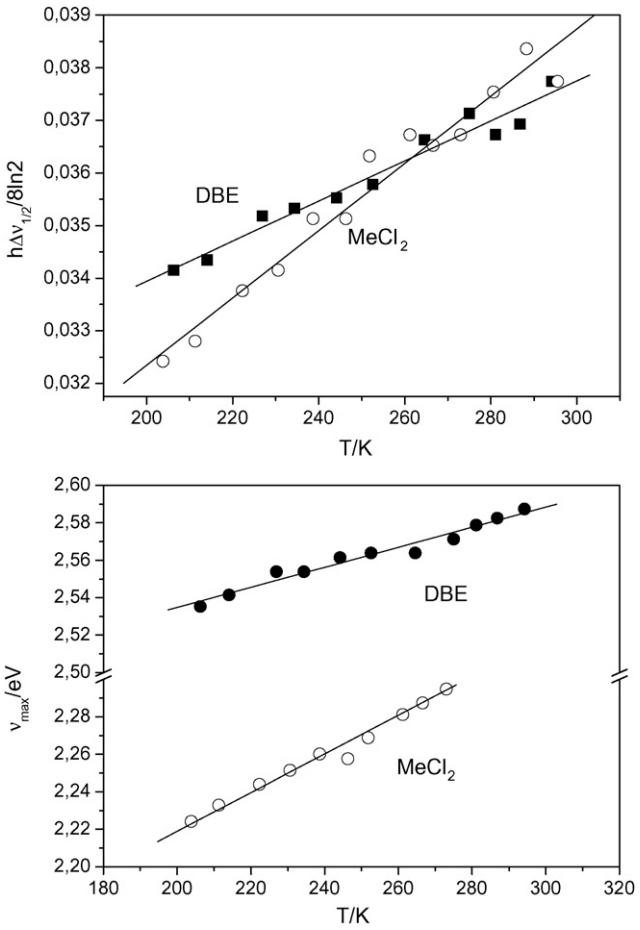

Fig. 9. Dependence of the halfwidth (top) and the position of the CT fluorescence maximum (bottom) on temperature for **II** in DBE and $MeCl_2$.

Analysis of the CT fluorescence measured at different temperatures yields also the parameters describing the back electron transfer process (the solvent reorganization energies and free energy changes) which are consistent with these parameters obtained for the solvents of different polarities at room temperature.

3.4. *trans–cis* isomerisation of the compound *II*

During our steady-state measurements we found that fluorescence intensity changes during the measurements. Moreover, the very strong dependence of the fluorescence lifetimes on temperature indicates an occurrence of the radiationsless process which deactivates the excited singlet state. It may be a *trans–cis* photoisomerisation which proceeds from the excited singlet state. Let us focus our attention to the compound **II** where a clear *trans–cis* isomerisation is observed. We performed the irradiation of the compound **II** in solvents of different polarity. Spectra of **II** irradiated by mercury lamp in acetonitrile are presented in Fig. 10.

We found that the irradiation of the solution of **II** in any solvent at 405 nm causes a decrease of the absorption band located approximately at 25,000 cm^{-1} (the position of the maximum depends on the solvent polarity) and an increase of the band at ca. 33,700 cm^{-1}. This corresponds to the *trans–cis* isomerisation of the dye. On the other hand, the irradiation at 313 nm causes a back reaction (i.e. *cis–trans* isomerisation). It indicates the reversibility of the *t–c* isomerisation process. For calculation of the *trans–cis* isomerisation quantum yields the following equation has been applied [15]:

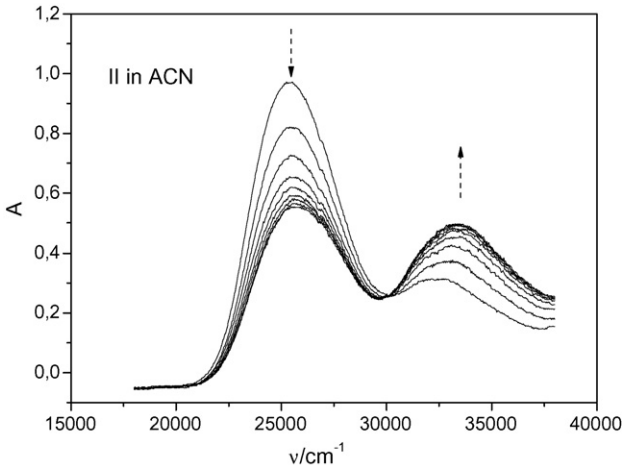

Fig. 10. Irradiation of solution of **II** in acetonitrile by a 405 nm line of the mercury lamp. Irradiation time spans the period 0–9 min with the 1-min intervals. The arrows indicate the decrease and increase of the appropriate absorption bands of *trans* and *cis* isomers.

$$\frac{dE}{dt} = QI(E - E_\infty)\frac{1 - 10^{-E'}}{E'} \quad (7)$$

where E denotes the absorption at the observation wavelength, E_∞ is the absorption extrapolated to the infinity irradiation time, whereas E' denotes the absorption at the irradiation wavelength. Q and I denote the pseudoquantum yield of photochemical process ($Q = \phi_1\varepsilon_1 + \phi_2\varepsilon_2$) and the intensity of the irradiation line, respectively. The parameters $\phi_{1,2}$ and $\varepsilon_{1,2}$ denote the partial quantum yields for *trans–cis* and *cis–trans* isomerisation and molar extinction coefficients of the isomer *trans* and *cis* at the excitation wavelength, respectively.

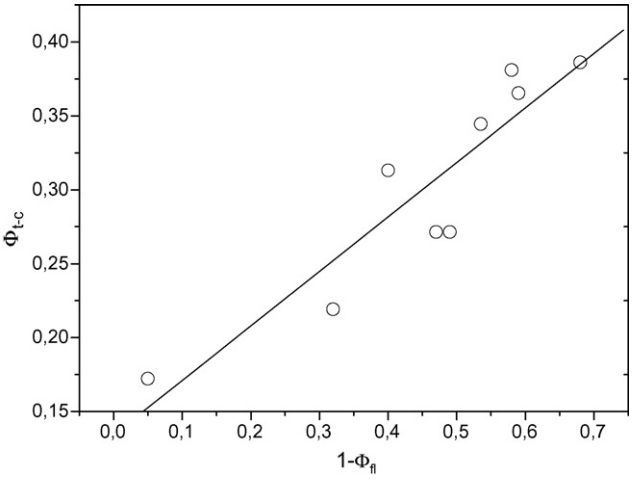

Fig. 11. Dependence of the *trans–cis* isomerisation quantum yield on the non-radiative quantum yield for the compound **II** in solvents of different polarities. The slope of the linear dependence is equal to 0.38 ± 0.06.

We have found that the quantum yield of the *trans–cis* isomerisation strongly depends on the polarity of the solvents. Moreover, this quantity correlates roughly linear with the quantum yield of nonradiative deactivation of the excited singlet state, as can be seen in Fig. 11.

4. Discussion

Absorption and fluorescence of unsubstituted 2-phenylbenzoxazole show a clear vibrational structure in the spectra, which smeares out when a double bond is attached (compound **I**). Further addition of the electron donating group (*N*,*N*-dimethylaniline) causes that the fluorescence has a strong charge transfer character. The dipole moment of the compound **II** in the ground state is equal to 5.75 D (*ab initio* calculation). In the excited singlet state the dipole moment is greatly enhanced (26.3 D) as can be judged from the very strong solvatochromic shift of the fluorescence spectra in solvents of different polarity. In the excited singlet state the molecule assumes a very strong charge transfer character. The fluorescence of these compounds may be analysed in terms of the radiative charge transfer theory yielding the parameters which characterize the back electron transfer process. The results were presented above in Figs. 5 and 6. The characteristic property of the dependence of λ_s on solvent polarity function is large values of the reorganization energies (up to 0.6 eV for the solvents of highest polarity) and the plot seems to saturate at lower polarity function values. This is somewhat expectable because the dipole change of the molecule upon excitation is very large. Noteworthy is the fact, that the internal reorganization energy (λ_{in}) seems to be solvent polarity dependent, it significantly decreases when solvent polarity increases. Similar behaviour has been found for the compound **III** with slightly larger values of λ_s for the same solvents. High fluorescence quantum yields may indicate that triplet population is not operative in the overall deactivation pathway of the singlet state. Indeed, the transient absorption spectra (not presented in the paper) rather exclude the formation of the triplet state of the dye. Thus, the deactivation pathways of the singlet state are radiative (fluorescence) and nonradiative transitions. We will show that the singlet state *trans–cis* isomerisation may be a dominant nonradiative pathway of the deactivation of the excited singlet state. First, having the CT parameters (λ_s, λ_{in}, ΔG_{et} and V_0) obtained from fluorescence band-shape analysis we are able to calculate the rate constants of nonradiative back electron transfer process. The calculated values of the nonradiative back electron transfer rate constants do not exceed a value of $2000\,s^{-1}$ in all cases, although the dependence of these quantities on ΔG_{et} is observed. Thus, we can conclude that the nonradiative back electron transfer process is not responsible for nonradiative transitions, because the electron transfer rate constants are around six order of magnitude smaller than the experimentally obtained nonradiative rate constants and the tendency of the change with changing solvent polarity is exactly opposite to the observed one. We observe decreasing of the rate constant with increasing solvent polarity whereas the calculated values show the opposite trend. This fact, with the observation that the population of the triplet state seems to be negligible, leads to the conclusion that the mayor nonradiative deactivation pathway of the fluorescing singlet state is the *trans–cis* isomerisation (Fig. 11).

This fact emerges from our data presented previously. First, we observe a large temperature dependence of the fluorescence lifetime on temperature as can be recognized from Fig. 8. At higher temperature the lifetimes are short (0.5 ns at 325 K) and increase rapidly when temperature decreases, up to the saturation at lowest temperatures close to the freezing point of ethyl acetate. Similar feature was observed in the fluorescence decay function measurements of **II** in methyl metacrylate, where the fluorescence lifetime was 0.93 ns but after polymerization the lifetime increased to 1.56 ns. Second, the internal conversion quantum yield correlates roughly linear with the isomerisation quantum yields as can be seen in Fig. 11. Very important seems to be the fact that internal reorganization energy decreases with increasing solvent polarity. This effect, not observed in the systems previously investigated by us (bianthryls), is not large but remarkable (cf. Fig. 6). The internal reorganization energy is connected with a change of the bond length and bond angles upon radiative electron transfer $S_1 \Rightarrow S_0$ process. A decrease of this quantity with increasing solvent polarity may suggest that in polar solvents the molecule has a contribution of the dipolar structure (presented below) already in the ground state. This dipolar structure exists exclusively in the fluorescing singlet state. Thus, electronic transition in polar solvents requires smaller intramolecular rearrangement compared to that in less polar solvents in which the contribution of the dipolar structure in the ground state is smaller.[2]

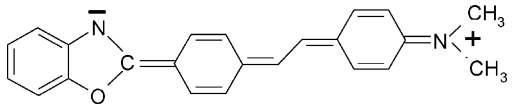

Inspection of Fig. 7 reveals that nonradiative transitions are more efficient in solvents of lower polarities, in which isomerisation is more effective. However, in solvents of similar polarities but with strongly different viscosities we observe an additional stabilisation (i.e. significantly smaller values of nonradiative rate constants). It may indicate that internal molecular motions leading to isomerisation are decellerated in viscous solvents (TGA and DMSO).

One important point emerges from the fluorescence observation of the system **IV** (containing azacrown ether). In acetonitrile an addition of the natrium (and barium) perchlorate causes a significant hypsochromic shift of the absorption spectra which may indicate to the formation of the host–guess complex, as it is presented in Fig. 12. However, the steady-state fluorescence spectra did not change significantly upon addition of the salt. We have performed the time-resolved measurements of the fluorescence. At the time-resolution of our system (70 ps) we could not detect any significant changes of the time-resolved spectra which may point out to the existence of the natrium (barium) complexes in the excited state. The dissociation of the cation complex (into

[2] In other words, so-called ground state ionicity, introduced by Painelli et al. [25] increases with increasing solvent polarity.

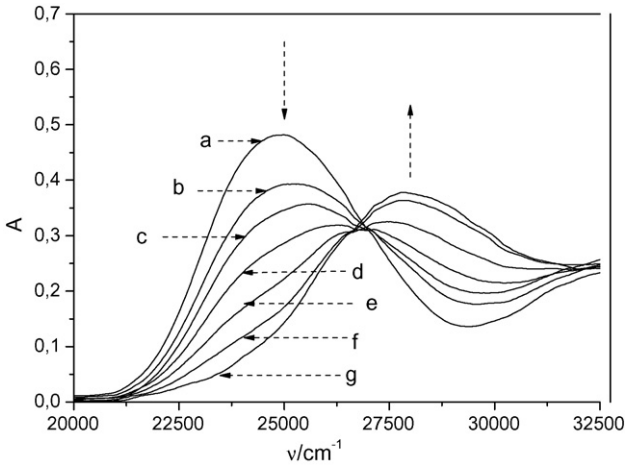

Fig. 12. Absorption spectra of **IV** in acetonitrile in the absence (a) and the presence of $Ba(ClO_4)_2$ of concentration 1.2×10^{-3} (b), 2.1×10^{-3} (c), 4.5×10^{-3} (d), 8.9×10^{-3} (e), $2. \times 10^{-2}$ (f) and 2.8×10^{-2} (g) M. The arrows indicate the decreasing (at 25,000 cm^{-1}) and formation (at 28,000 cm^{-1}) of the new absorption band of the barium cation containing system.

excited dye and the cation) in the excited state is then faster than our time resolution of the system. Similar behaviours have been reported and explained in literature [26]. The system is therefore not appropriate as a fluorescence indicator of small inorganic cations.

5. Conclusions

The fluorescence properties of the four dyes based on the benzoxazole skeleon have been investigated. Introduction of the dimethylamine into the phenyl ring causes a significant enhancement of the charge transfer character in the first excited singlet state (compounds **II**–**IV**). The compound **II** was investigated in detail in respect of the *trans–cis* isomerisation. It has been found that for this compound the isomerisation is commenced in the excited singlet state. This is validated on the basis of the proportionality of the isomerisation and the nonradiative quantum yields. The internal conversion rate constants depend on the two physical factors: viscosity and polarity of the solvents, however most important is the polarity factor. The molecules (**II**–**IV**) may be used as fluorescence indicator tracing the progress of polymerization.

Acknowledgements

This work was supported by the State Committee of Scientific Research of Poland (Grants No 3 T09A 102 18 and 4T09A 109 25). We would like to thank Prof. Jan Najbar for diverse help in the course of completion of this project and Dr. Andrzej M. Turek for editorial comments.

References

[1] M.H. Keefe, K.D. Benkstein, J.T. Hupp, Coord. Chem. Rev. 205 (2000) 201.
[2] H.R. Hoveyda, S.J. Rettig, C. Orvig, Inorg. Chem. 32 (1993) 4909.
[3] M.B. Reynolds, M.R. DeLuca, S.M. Kerwin, Bioorg. Chem. 27 (1999) 326.
[4] C.-W. Ko, Y.-T. Tao, A. Danel, L. Krzemińska, P. Tomasik, Chem. Mater. 13 (2001) 2441.
[5] J. Saltiel, Y.-P. Sun, in: H. Duerr, H. Bouas-Laurent (Eds.), Photochromism—Molecules and Systems, Elsevier, Amsterdam, 1990, p. 64.
[6] D.H. Waldeck, Chem. Rev. 91 (1991) 415.
[7] K. Rechthaler, G. Köhler, Chem. Phys. Lett. 250 (1996) 152.
[8] Y.V. Ill'ichev, W. Kühnle, K.A. Zachariasse, Chem. Phys. 211 (1996) 441.
[9] G. Gurzadyan, H. Görner, Chem. Phys. Lett. 319 (2000) 164.
[10] T.A. Fayed, S.E-D.H. Etaiw, H.M. Khatab, J. Photochem. Photobiol. A: Chem. 170 (2005) 97.
[11] T.A. Fayed, J. Photochem. Photobiol. A: Chem. 121 (1999) 17.
[12] A.E. Siegrist, Helv. Chim. Acta 50 (1967) 907.
[13] M. Mac, P. Kwiatkowski, A.M. Turek, J. Lumines. 65 (1996) 341.
[14] H. Gőrner, Ber. Bunsenges. Phys. Chem. 102 (1998) 726.
[15] G. Gauglitz, S. Hubig, J. Photochem. 30 (1985) 121.
[16] E. Lippert, Z. Naturforsch. 10a (1955) 541;
N. Mataga, Y. Kaifu, M. Koizumi, Bull. Chem. Soc. Jpn. 28 (1955) 690.
[17] A. Kawski, Z. Naturforsch. 57a (2002) 255.
[18] J.F. Rabek, Progress in Photochemistry and Photophysics, vol. V, CRC Press Inc., 1992.
[19] S.L. Murov, Handbook of Photochemistry, Marcel Dekker, Inc., New York, 1973, p. 85.
[20] R.A. Marcus, J. Phys. Chem. 93 (1989) 3078.
[21] I.R. Gould, R.H. Young, L.J. Mueller, A.C. Albrecht, S. Farid, J. Am. Chem. Soc. 116 (1994) 8188;
I.R. Gould, R.H. Young, R.E. Moody, S. Farid, J. Phys. Chem. 95 (1991) 2068.
[22] P. Borowicz, J. Herbich, A. Kapturkiewicz, M. Opallo, J. Nowacki, Chem. Phys. 249 (1999) 49.
[23] J.E. Lewis, M. Maroncelli, Chem. Phys. Lett. 282 (1998) 197.
[24] J. Cortes, H. Heitele, J. Jortner, J. Phys. Chem. 98 (1994) 2527.
[25] A. Painelli, F. Terenziani, Chem. Phys. Lett. 312 (1999) 211.
[26] B. Valeur, Molecular Fluorescence, Wiley–VCH, Weinheim, 2002, p. 299.